Therapeutic targeting of SETD2-deficient cancer cells with the small-molecule compound RITA

Kirsten A. Lopez, Deborah Sneddon, Sovan Sarkar, Oliver Busby, Elena Seraia, Chiara Toffanin, Christian Cooper, Michalis Challoumas, Fiona A. Okonjo, George D. D. Jones, Francesca Buffa, Daniel Ebner, Jennifer A. Ward, Felix Feyertag, Kilian V. M. Huber, Bart Cornelissen, Stuart J. Conway, and Timothy C. Humphrey

Supplementary Data

Table S1. List of compounds in the Oncology Drug Library (ODL) and Selleck Library that were included in the high-throughput screen.

Table S2. CETSA analysis of proteins affected by RITA in SETD2-deficient U2OS cells. List of top Destabilized GO Terms; All proteins and replication stress proteins

Supplementary Figures S1-S14; Schemes S1-6; Supplementary RITA variant synthesis details.

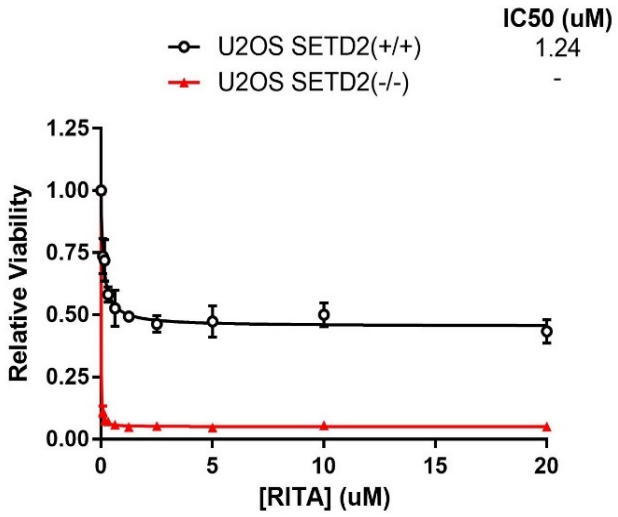

Fig. S1. Dose-response viability curve for RITA in parental and SETD2-CRISPR U2OS cells. Data are shown as mean ± SD (n ≥ 4). IC50 values were calculated via nonlinear regression (4-parameter curve fitting) when possible.

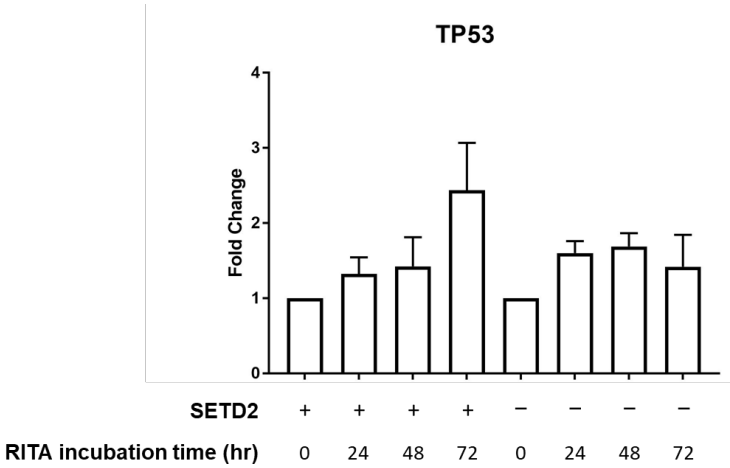

Fig. S2. Quantitative RT-PCR analysis of TP53 gene expression after RITA treatment. Samples were normalised to the housekeeping gene GAPDH. Fold change was calculated relative to untreated controls. Data are shown as mean ± SD.

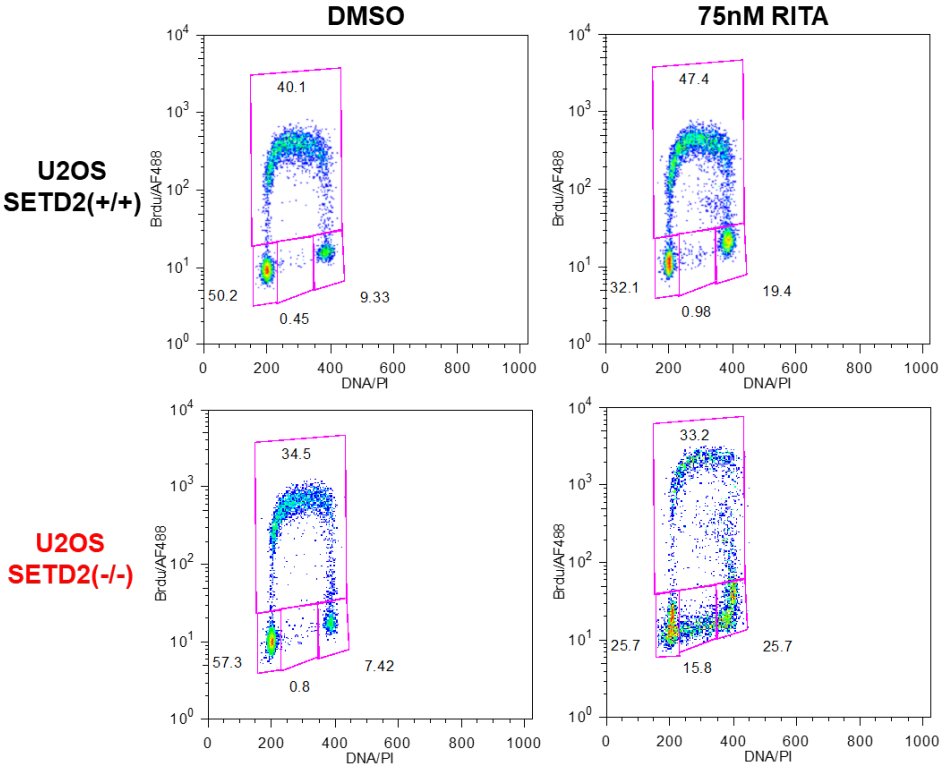

Fig. S3. BrdU/PI cell cycle profiles of U2OS cells after DMSO or RITA treatment. Images are representative of 3 independent experiments.

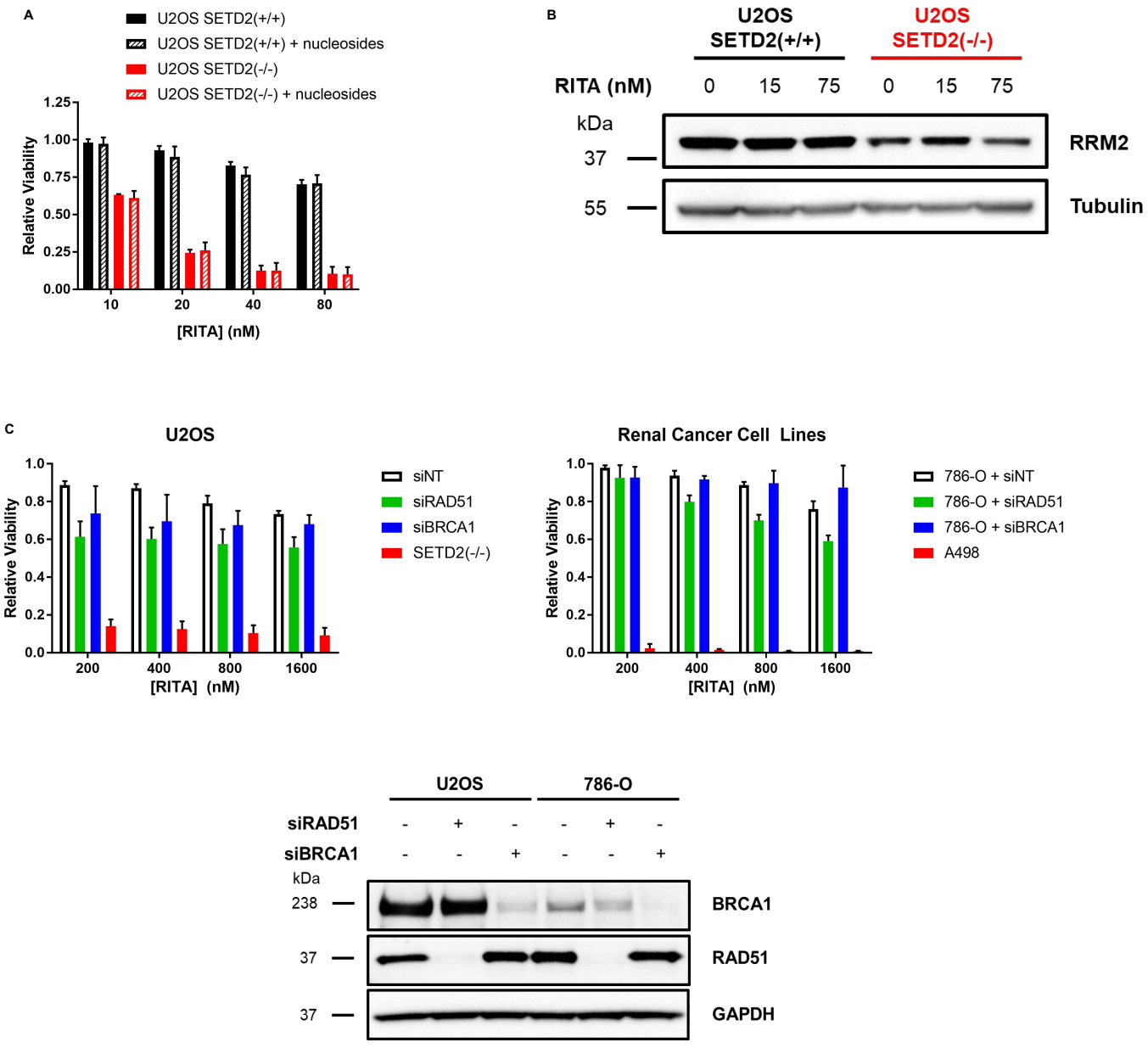

Fig. S4. RITA sensitivity of SETD2-deficient cells is not associated with nucleotide pools or homologous recombination. **(A)** Cell viability assay after RITA treatment of U2OS cells in the presence or absence of exogenous nucleosides. Data are shown as mean ± SD (n = 3). **(B)** Western blot of RRM2 protein in parental and SETD2-CRISPR U2OS cells treated with the indicated doses of RITA for 24 hours. **(C)** Cell viability assay after RITA treatment of U2OS cells or 786-O cells transfected with non-targeting (NT), RAD51, or BRCA1 siRNA. Data are shown as mean ± SD (n = 3). siRNA knockdown efficiency was confirmed by Western blot.

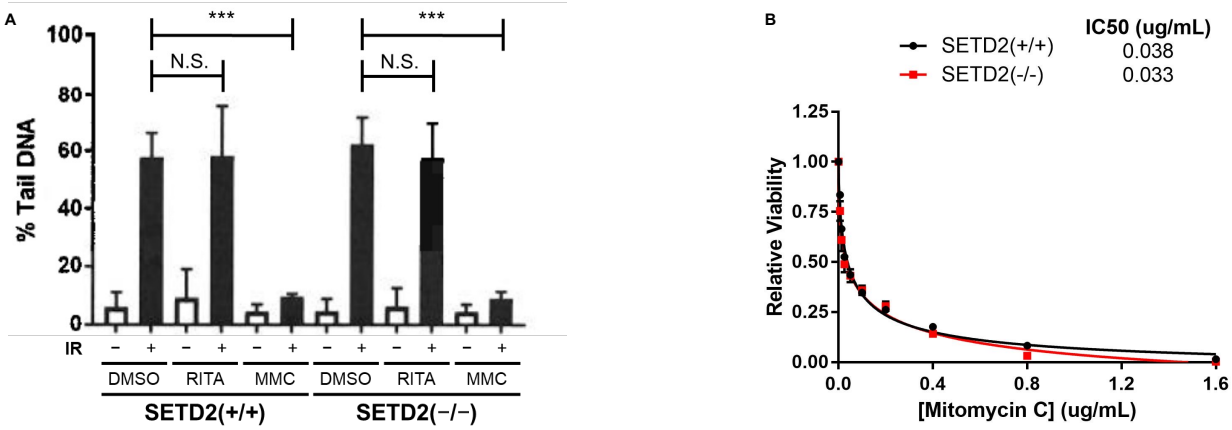

Fig. S5. RITA sensitivity in the absence of SETD2 is not associated with DNA crosslink formation. **(A)** Amount of fragmented (tail) DNA after ionising radiation (IR) as measured by comet assay in U2OS cells treated with RITA or mitomycin C (MMC). Data are shown as mean ± SEM (n = 3), each with 3 slides where 100 comets were counted per slide. P-values were calculated using the Student's two-tailed t-test. *** $p < 0.001$, N.S. = non-significant. **(B)** Dose-response viability curves for mitomycin C in U2OS cells. Data are shown as mean ± SD (n = 3). IC50 values were calculated via nonlinear regression (4-parameter curve fitting).

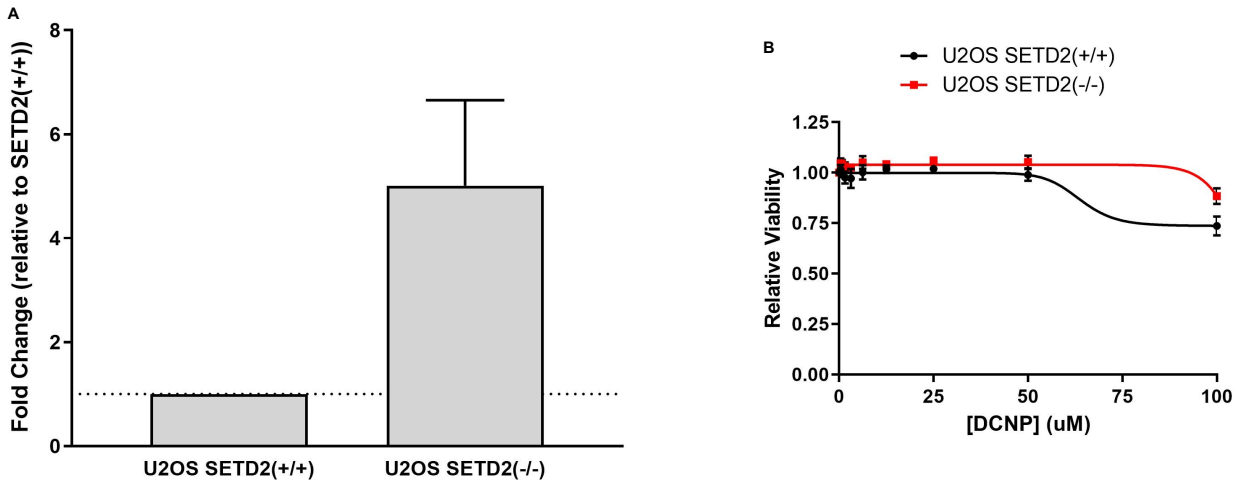

Fig. S6. RITA sensitivity in the context of SETD2 loss is correlated with expression levels of the phenol sulphotransferase SULT1A1. **(A)** Quantitative RT-PCR analysis of *SULT1A1* gene expression in U2OS cells. Samples were normalised to the housekeeping gene *GAPDH*. Fold change was calculated relative to wild-type SETD2(+/+) U2OS. Data are shown as mean ± SD. **(B)** Dose response viability curves for U2OS cells treated with the phenol sulphotransferase inhibitor DCNP. Data are shown as mean ± SD.

Introduction to RITA analogues:

Previously, analogues of **RITA** (Fig. S7) were prepared by groups interested in **RITA** as an inhibitor of the tumour suppressor protein p53.[1–4] It was proposed that **RITA** binds to the *N*-terminal transactivation domain of TP53, blocking MDM2/HDM2-TP53 binding.[1,5–7] Through ^{14}C-labelled RITA, Rivera *et al.* determined that the sensitivity of **RITA** directly correlated to: (i) the uptake and retention of the compound, and (ii) the ability of cell lines to metabolize **^{14}C-RITA** to a reactive species able to bind covalently to cellular macromolecules.[8]

Jiang *et al.*[1] and Lin *et al.*[2] examined several triheterocyclic variants, altering the heteroatoms and substituents. In both studies, they found that replacing the central furan for thiophene (**RV-15,** ; Fig. S7) generally resulted in an increased antiproliferative effect across several cell lines tested (K562, MCF-7, A549, HCT116), concluding that the sulfur atoms are a key factor determining antiproliferative activity.[1,2] Pietkiewicz *et al.* suggested this increase in activity is due to thiazoles having a larger aromatic character compared to furans, increasing the potential for π-stacking with target proteins.[3] Jiang *et al.* examined replacing the terminal hydroxymethyl substituents in **RITA** with several groups including: formyl (**RV-6**), acetyl and 2-methyl-1,3-dioxolanyl (**RV-16**) groups, with **RV-16** demonstrating greater antiproliferative activity compared to **RITA** in the majority of cell lines (MCF-7, A549, HCT116).[1] The structure activity relationship of the other tested substituents was less clear and appeared to be cell line dependant.[1] Lin *et al.* examined mixed substituent variants (e.g. **RV-17**, Fig.S7) and intermediates of **RITA**.[2] They determined that the general order of antiproliferative activity was **RITA**>**RV-17**>**RV-6** in the cell lines tested (K562, MCF-7, A549, HCT116, but not HCT116/*p53*$^{-/-}$) and considered that the hydrophilic hydroxymethyl group may hydrogen bond with the target, resulting in improved pharmacokinetic properties.[2]

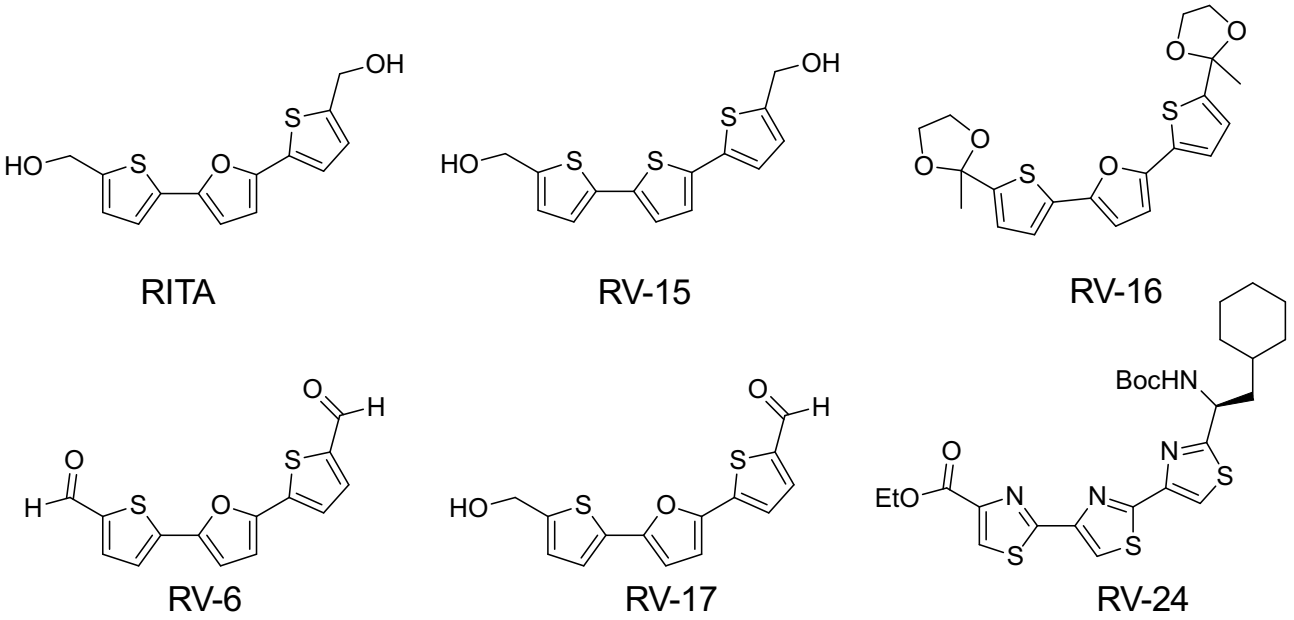

Fig. S7. Examples of previously prepared triheterocyclic compounds for p53 inhibition

The McAlpine[3] and Wipf groups[4] also explored structural variants of **RITA**. McAlpine examined a range of oxazole and trithiazole analogues (41 total), replacing the terminal substituents with groups of varying steric bulk.[3,9] All molecules were tested for the ability to inhibit the growth of HCT116 cells, with their lead compound **RV-24** (Fig. S7) acting in a distinct mechanism from **RITA**.

Wipf's group synthesized a range of furan, thiophene and selenophene regioisomers (Fig. S8), in addition to isosteric replacements of the terminal thiophene groups with oxazoles.[4] These new analogues were tested in NCI 60-cell line panel for selective anticancer activity and found that compounds RV-20 to RV-22 were the most potent, in general being more toxic to the renal cell line A498.[4] Although these studies provide more information on the SAR of RITA analogues, the uptake, specificity and mechanism of action remained unclear.

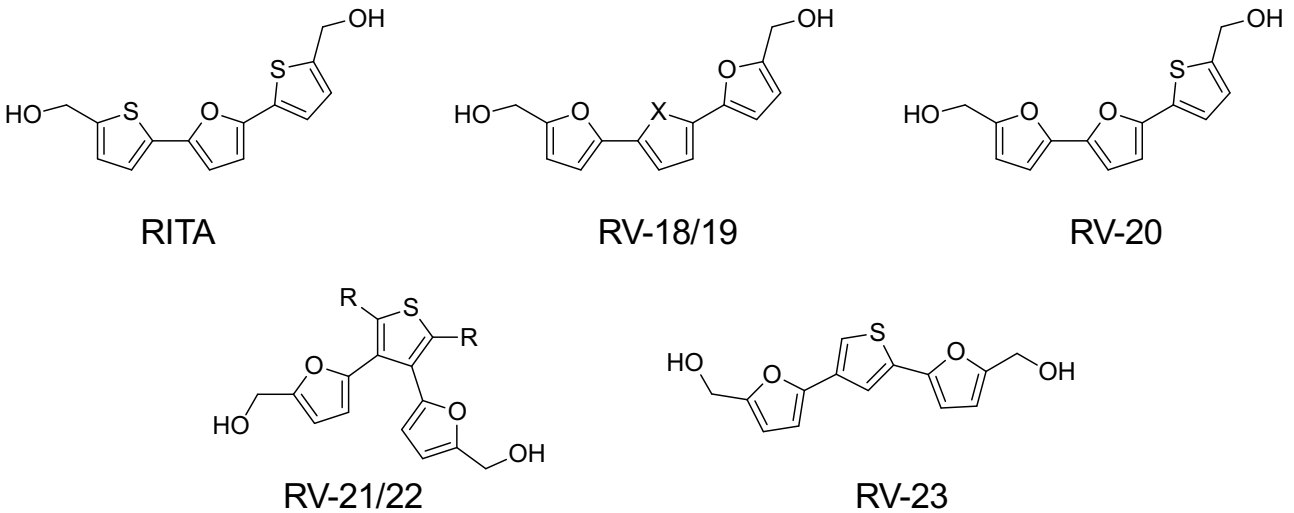

Fig. S8 . Lead compounds examined by Wipf and co-workers.[4]

RITA sulfation:

Previously, **RITA** was shown to be a SULT1A1 substrate that was sulfated by recombinant SULT1A1 *in vitro.*[10] Peyser, Wipf and coworkers suggested that the activity of **RITA** is as a result of a sulfation and elimination to a reactive carbocation species, similar to 1-hydroxymethylpyrene (HMP), (Fig. S9), rather than TP53 expression.[7] The presence of hydroxymethyl groups are key for this reaction, and explains the general trend in antiproliferative activity from hydroxymethyl>aldehyde. They examined the lead compounds from their initial screen (Fig. S8) and found that changing the arrangement of the heterocyclic core enabled cell line hyperselectivity, remaining potent against A498 cells.[7]

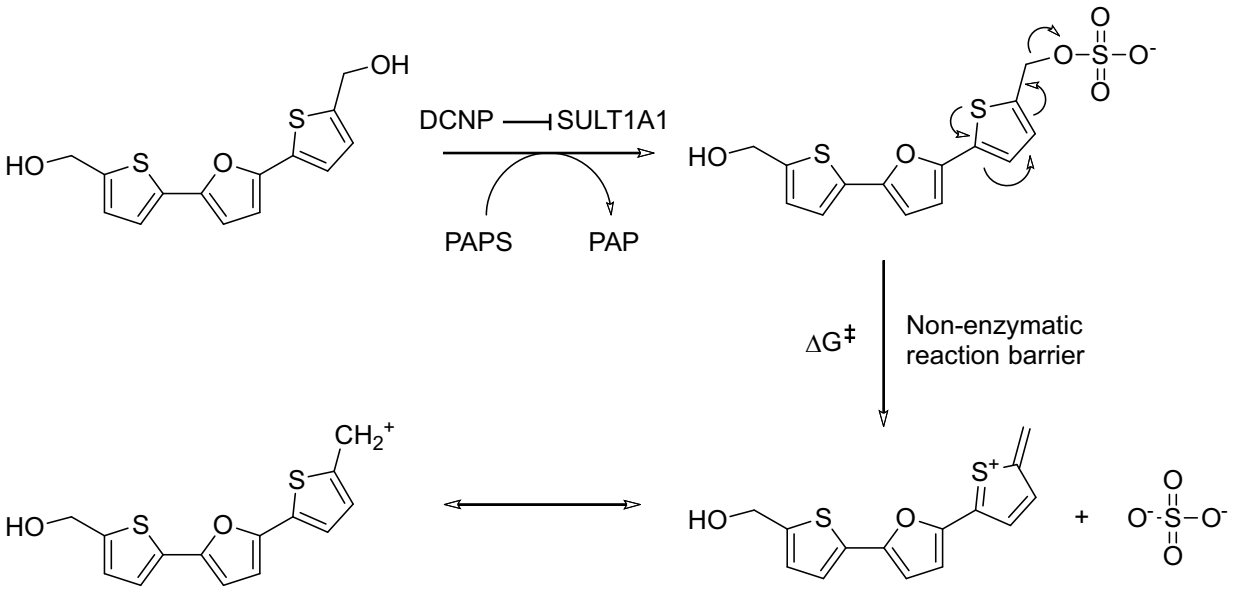

Fig. S9. Proposed sulfation of RITA via SUL1A1 with 3′-phosphoadenosine 5′-phosphosulfate (PAPS) and 3′-phosphoadenosine 5′-phosphosphate (PAP) cofactor as suggested by Wipf and co-workers[7] based on the sulfation of HMP.[11] Wipf and co-workers found that activity of RITA is supressed by phenol sulfotransferase inhibitor 2,5-dichloro-4-nitrophenol (DNCP). [7]

Peyser and Wipf postulate that the broad cytotoxicity observed for RITA and nonspecific DNA/protein crosslinking is due to the reactive carbocation formed, but note that the changes to the heterocyclic core of RITA result in differences in tumour cell line toxicity and selectivity.[7] Addition of phenol sulfotransferase inhibitor 2,5-dichloro-4-nitrophenol (DNCP) abrogated activity of **RV-18** in NCI-60 cells, but surprisingly, the authors found that cell line NIH-H460, which expresses the highest level of SULT1A1 mRNA, was resistant to **RV-18**. The authors suggested that there may be a requirement for specific target(s) in addition to metabolic activation, but the transition state barrier for the spontaneous formation of a carbocation remains a key indicator of broad activity.[7]

Following on from this work, Zhan *et al.* re-examined compounds **RV-20** and **RV-23** (Fig. S8) against **RITA** to determine if they could induce p53-dependant apoptosis without the associated SULT1A1 DNA damage.[12] Differences in the SULT1A1 dependence of **RV-20** and **RV-23** were apparent, as were the mechanisms resulting in oncogene repression. They concluded that analogue **RV-23** was specifically targeting p53 in cancer cells.[12]

Clearly, the exact mechanism of **RITA** action remains to be elucidated, and it is likely that several mechanisms contribute to the cytotoxic effect. It has been demonstrated that small structural variants contribute to cancer cell specificity, therefore we were interested in testing novel **RITA** variants in SETD2 deficient cancer cells.

New RITA variants:

As described by several groups, the terminal hydroxyl groups are key to **RITA** binding to p53.[2,6,7] Lin *et al.* identified that replacing the alcohol group of **RITA** either with an aldehyde or TDMS protecting group resulted in decreased cell death in p53 wild type HCT116 cells and suggested that **RITA** may hydrogen bond to the target.[2] Grinkevich *et al.* proposed an allosteric mechanism, and determined that hydrogen bonding of the alcohol groups of **RITA** to serine 33 and 37 in the N-terminal binding domain of p53 were crucial in binding of **RITA** to p53.[6] Through Monte Carlo simulations, their model additionally implied hydrophobic interactions via one of the thiophene and the furan ring with proline 34 and 36.[6] Grinkevich *et al.*[6] suggested that in their model, the furan ring is not relevant to binding to p53 and that it could be substituted for a different heteroatom (thiophene), experimentally shown by Jiang, Lin, and Wipf.[1,2,7]

We considered the metabolism of **RITA**, through alcohol dehydrogenase (ADH) and aldehyde dehydrogenase (ALDH2) to a carboxylic acid (Figure S11).[13] Although these polymorphic enzymes are expressed at the highest levels in the liver, they are found in lower levels in many tissues.[13] Once converted to the aldehyde by ADH, rapid conversion to the corresponding carboxylic acid is expected. The proposed carboxylic acids would undergo hydrogen bonding to serine 33 and 37 as for **RITA** (Figure S12) but would not undergo sulfation and elimination to the **RITA**-like carbocation. As the cell membrane permeability of the carboxylic acid variants would be compromised, we proposed protecting the carboxylic acids with esters, which could be removed *in vitro* due to esterase activity.

Grinkevich *et al.* analysed **RITA** analogues and concluded that three rings (but not necessarily the central furan) were necessary for their p53 biological activity.[6] The analogues compared include tetrad thiophenes, pyrrole systems and others.[6] To the best of our knowledge, a thiophene dyad **RITA** analogue has not been analysed. A dyad offers synthetic simplicity in comparison to the triad system and could retain the hydrophobic interaction with prolines 34 and 36.

Synthesis and Analysis of RITA variants:

A small panel of **RITA** analogues were prepared (Fig. 6) functionalised with dual aldehydes (**RV-6**), dual methyl esters (**RV-12**) and a mixed aldehyde/methyl ester (**RV-11**). Two thiophene dyads with dual aldehyde and hydroxylemthyl groups (**RV-13** and **RV-14** respectively) were also prepared. Compound **RV-13** was previously isolated as a major byproduct by Lin *et al.*,[2] but to the best of our knowledge, the antiproliferative activity of this compound was not analysed.

The compounds were prepared in broadly the same manner as has been previously reported by Lin *et al.*[2] utilizing Suzuki coupling strategies (full details given below). RITA analogues (Figure 6) and selected intermediates were examined in U2OS SETD2 (+/+) and (-/-) cells (Fig. S10). **RITA** demonstrated a striking effect on cell viability in SETD2 (-/-) cells compared to SETD2 (+/+) cells as described (Fig. 6; Fig. S10A), with the dialdehyde variant **RV-6** being less active (Fig. 6), following the pattern described by Jiang and Lin *et al.*[1,2]

If our mechanism for alcohol oxidation via ADH and ALDH2 to a carboxylic acid was correct, we would expect that the dialdehyde **RV-6** could also undergo this mechanism. Aldehydes can easily diffuse across cell membranes and can form adducts with plasma membrane proteins,[14] which may account for its limited activity. However, the dual methyl ester **RV-12** showed no activity in U2OS SETD2 (+/+) and (-/-) cells (Fig. S10C) which was recovered slightly for the mixed methyl ester/aldehyde compound **RV-11** (Fig. S10B) only at concentrations at 1 μM. It may be that these compounds have different uptake and retention mechanisms in comparison to **RITA**, resulting in their poor toxicity profile, however, it is more likely that these compounds cannot be sulfated by SULT1A1 and cannot undergo the subsequent elimination to the carbocation species.

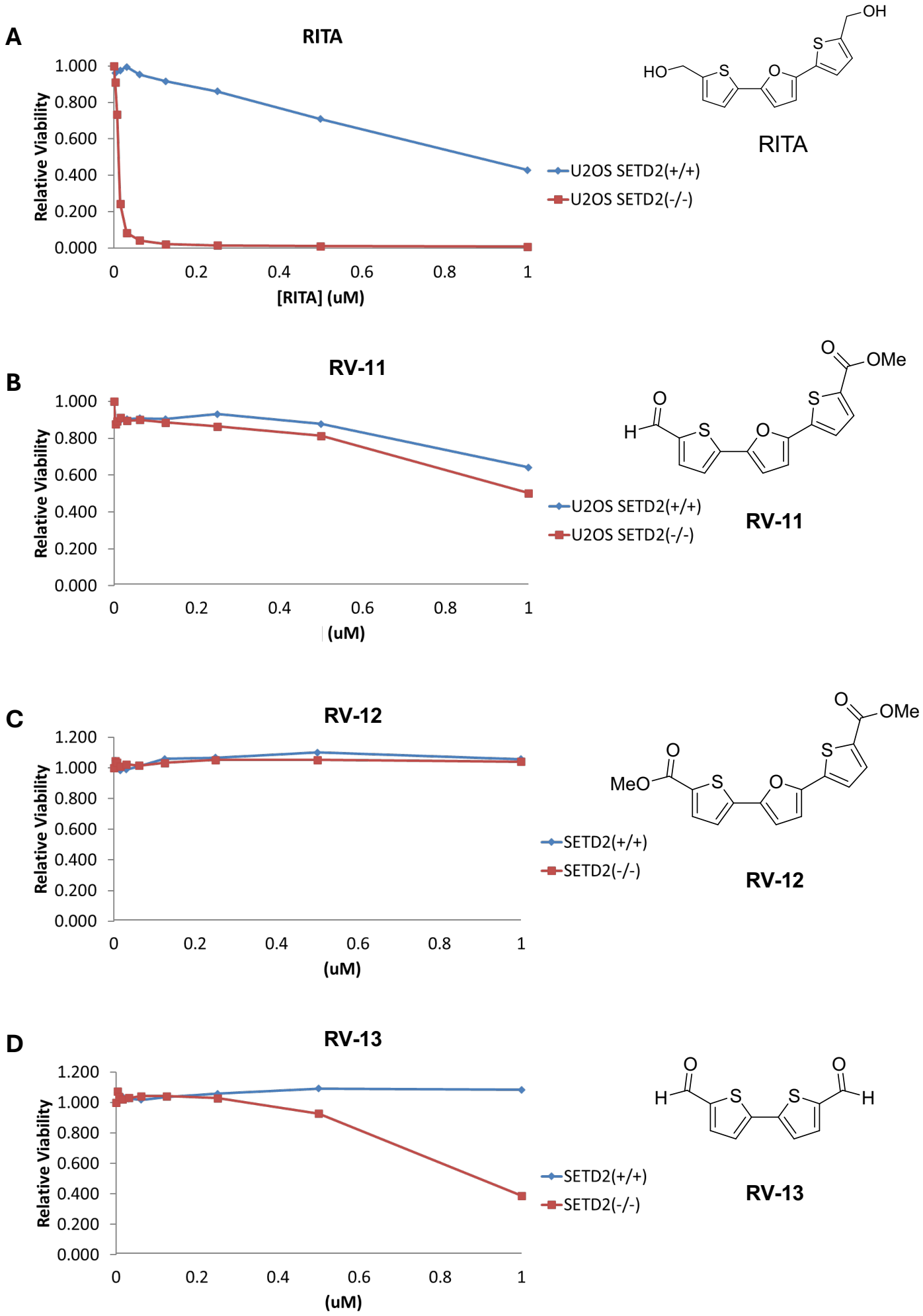

Figure S10. Cell viability curves for RITA analogues, n=3

In comparison, the dyad compounds **RV-13** and **RV-14** did show an increased cytotoxicity in U2OS SETD2 (-/-) cells compared to SETD2 (+/+) cells (Fig. S10D and Fig 6C). The dyad **RV-14** (Fig.6) bearing the two hydroxyl substituents was more cytotoxic in U2OS SETD2 (-/-) cells than the aldehyde dyad **RV-13** (Fig. S10D), following the same trend as for **RITA** and compound **RV-6**. Higher concentrations of **RV-14** were necessary to invoke the same cell death in U2OS SETD2 (-/-) cells compared to **RITA**, suggesting that a central heterocyclic ring results in favourable toxicity. The relative viability of U2OS SETD2 (+/+) cells treated with **RV-14** was approximately 100%, compared to 50% for **RITA**. Dyad **RV-14** may be more selective for U2OS SETD2 (-/-) cells but the relative cytotoxicity is similar to dialdehyde **RV-6**. The general order of activity is **RITA** > **RV-6** ≈ **RV-14** > **RV-13**.

The cell viability of selected intermediates (Fig.S13) of these analogues was also examined (Fig. S14), but generally the intermediate showed similar toxicity to both cell lines with no significant difference with the exception of 5-(5-bromofuran-2-yl)thiophene-2-carbaldehyde (**RV-2**). Compound (**RV-2**) showed some selectivity for U2OS SETD2 (-/-) cells at higher concentrations (Fig. S14B), with a profile similar to **RV-13** (Fig.S10D).

The **RITA** analogues tested confirmed that a central heterocyclic ring improved cytotoxicity in U2OS cells and corroborated previous work that hydroxymethyl substituents were important to confer cytotoxicity.[1–3,12] The selectivity between SETD2 (+/+) and (-/-) cells is likely due to the significant upregulation of SULT1A1 in SETD2 (-/-) cells, resulting in sulfation followed by elimination of the hydroxymethyl substituents.

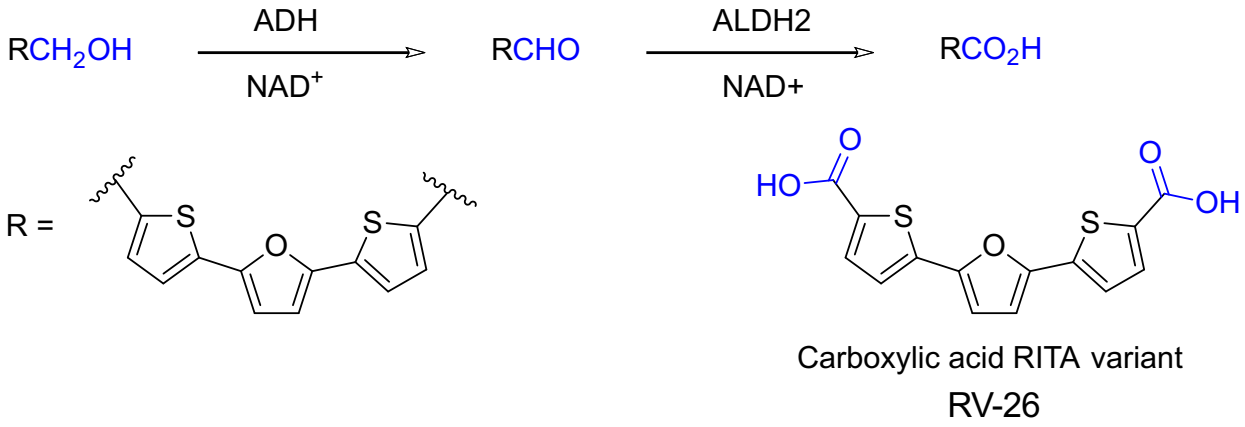

Figure S11. Proposed metabolism of RITA compounds via alcohol dehydrogenase (ADH) and aldehyde dehydrogenase (ALDH2) to carboxylic acids.

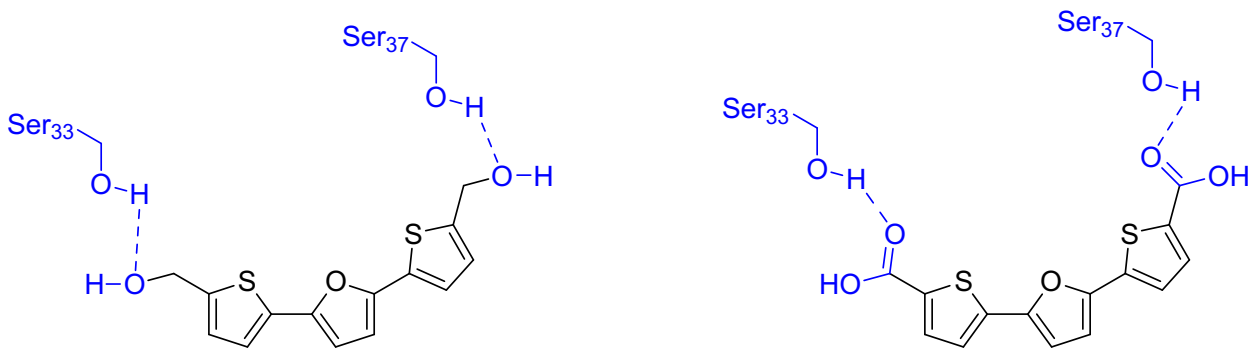

Figure S12 . Proposed hydrogen bonding of carboxylic acid RITA variant **RV-26** to serine residues 33 and 37 of p53.

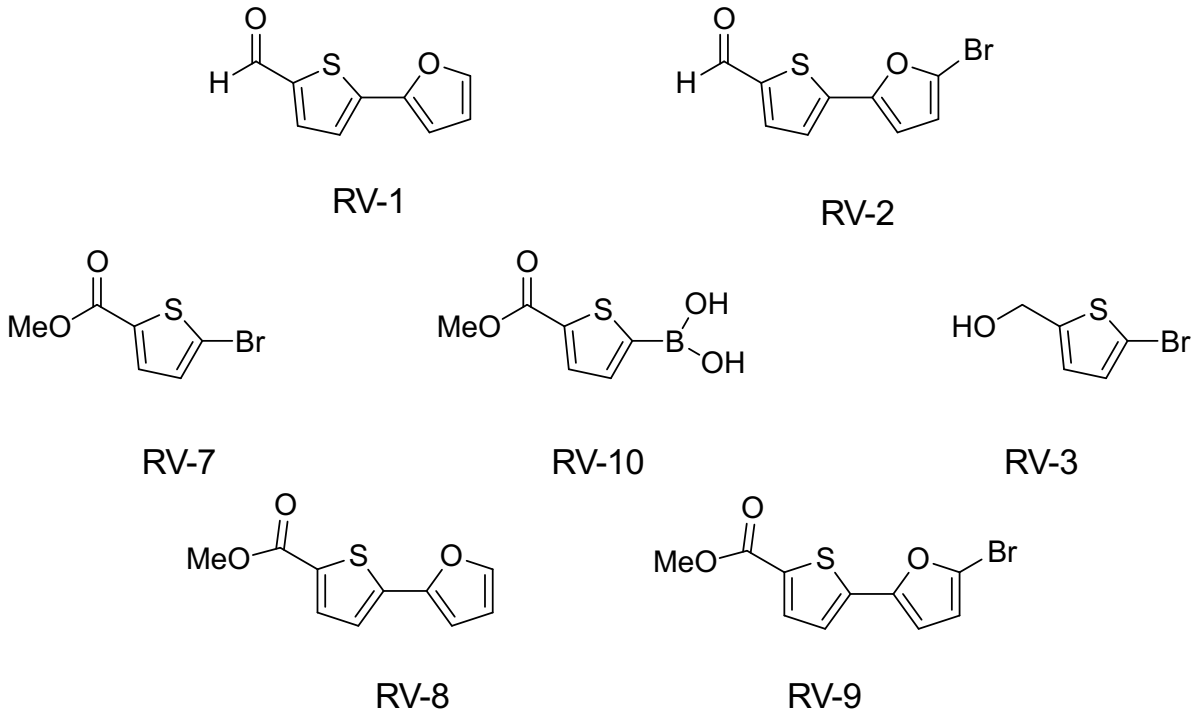

Figure S13. Selected RITA intermediates examined for cell viability

A

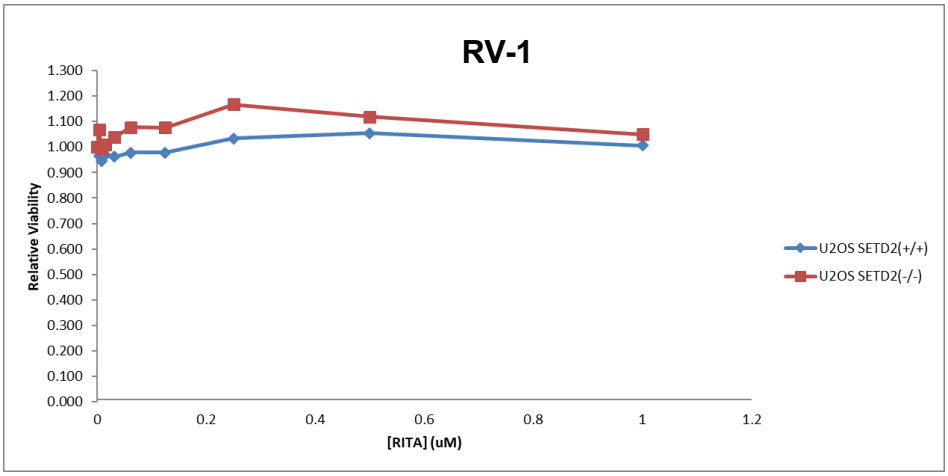

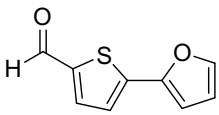

RV-1

B

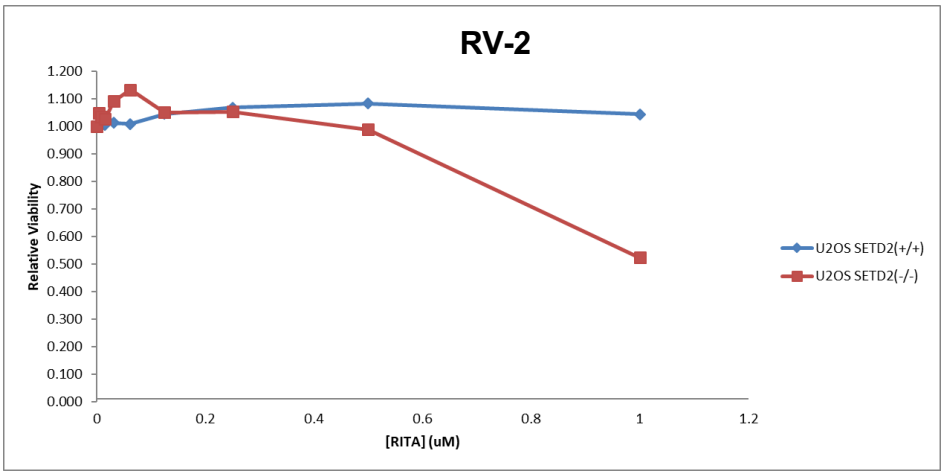

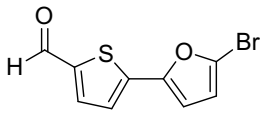

RV-2

C

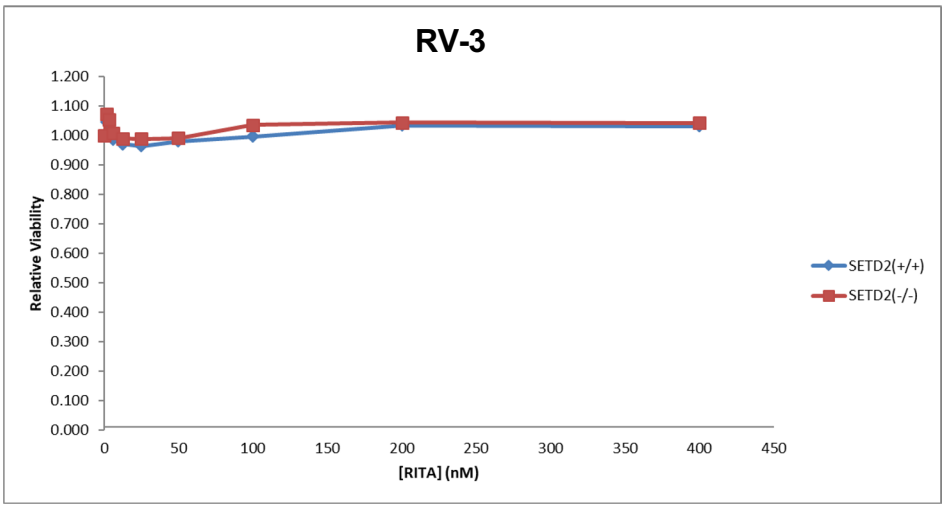

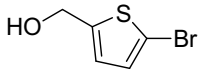

RV-3

D

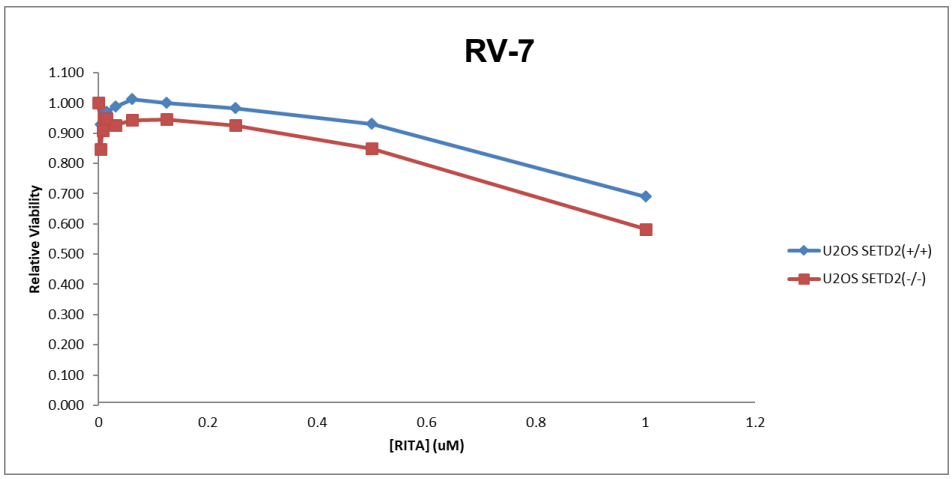

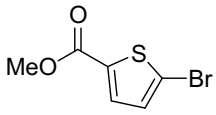

RV-7

E

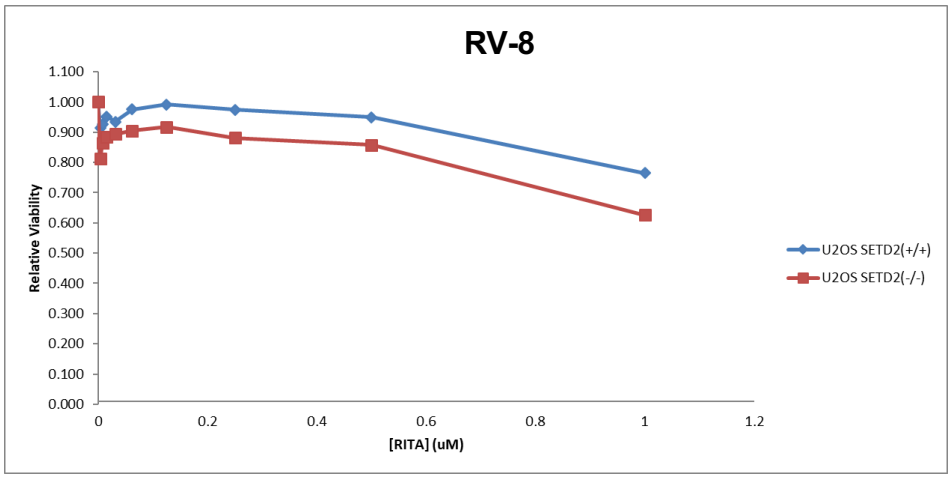

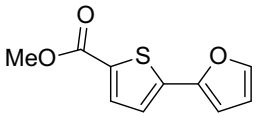

RV-8

F

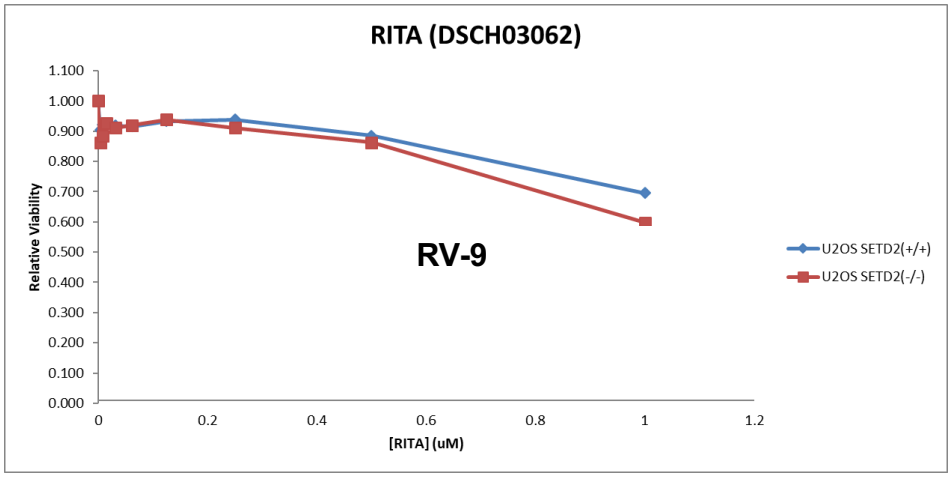

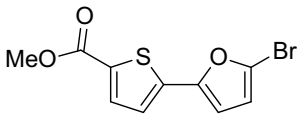

RV-9

G

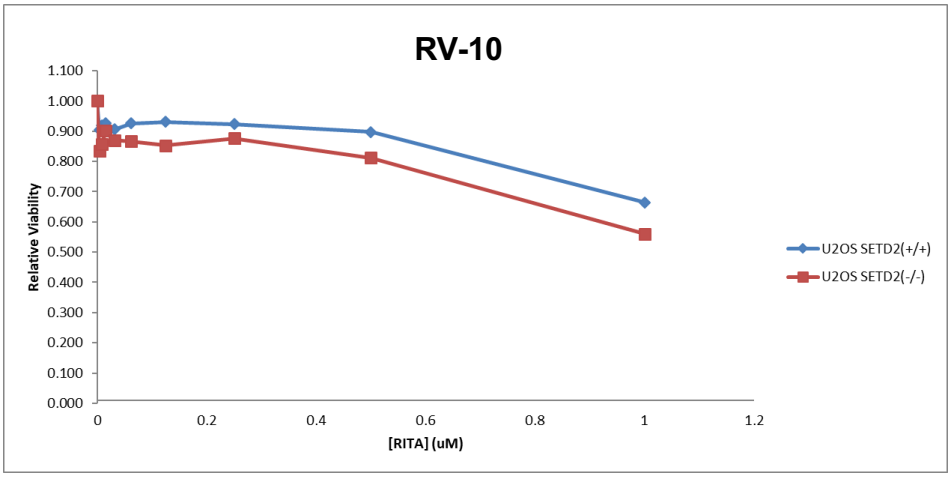

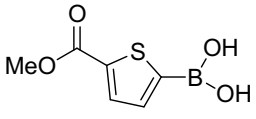

RV-10

Fig. S14. Cell viability for **RITA** analogue intermediates n U2OS SETD2 (+/+) and U2OS (-/-) cells.

Synthesis of further RITA variants:

The synthesis of novel **RITA** analogues were prepared in broadly the same manner as has been previously reported by Lin *et al.*[2] for RITA utilizing Suzuki coupling strategies (Scheme S1).

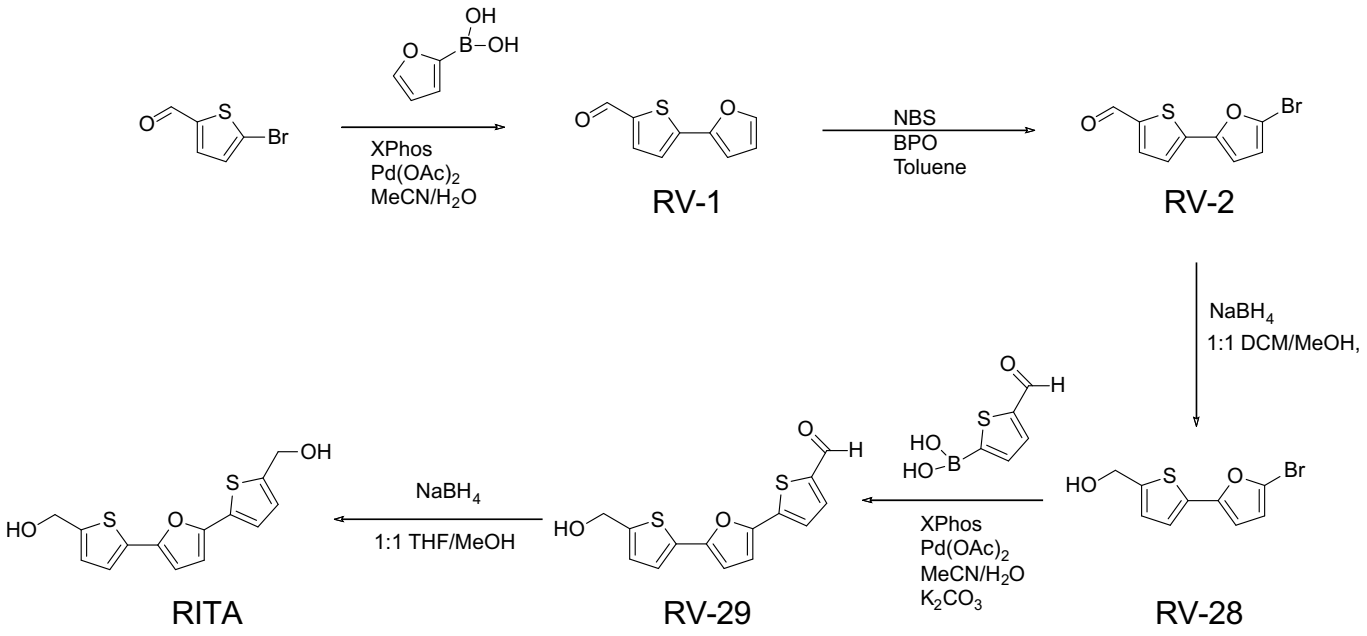

Scheme S1. Lin *et al.* method for synthesizing **RITA**[2]

In brief, 5-bromo-2-thiophenecarboxaldehyde was combined in degassed MeCN/H_2O (1.5:1) with XPhos (0.02 eq.) and $Pd(OAc)_2$ (0.01 eq.) and K_2CO_3 (3 eq.). To this, 2-furanylboronic acid (1.5 equiv) was added and the reaction was allowed to stir at room temperature overnight. 5-(furan-2-yl)thiophene-2-carbaldehyde (**RV-1**) was obtained by column chromatography in a moderate yield (24-70 %, n=7). The addition of bromine to the **RV-1** was achieved by radical chemistry using benzoyl peroxide and *n*-bromosuccinimide in toluene at -15 °C in the dark. After 3 h, the reaction was determined to be complete by TLC despite the starting material and product having very similar retention times. Low yields were initially obtained for this reaction any heating (upon solvent removal *in vacuo* for example) would result in what was assumed to be polymer formation. This was quickly indicated from the yellow/orange crystalline powder rapidly turning black when heated. Despite this, when kept at room temperature or at -20 °C and in powder form, the 5-(5-bromofuran-2-yl)thiophene-2-carbaldehyde (**RV-2**) remains relatively stable and could be isolated in moderate yield (49-70%, n=7).

The starting material 5-bromo-2-thiophenecarboxaldehyde, **RV-1** and **RV-2** can be reduced to their corresponding alcohols **RV-3**, **RV-27** and **RV-28** using $NaBH_4$ (0.5 eq.). Compound **RV-28** was one of the key intermediates of Lin *et al.* but they noted that compounds had to be used as soon as possible due to instability. We also found these compounds to be unstable and in the synthesis of **RITA** (following Scheme S1), generally **RV-28** was used without further purification or analysis assuming 100% yield, but in in our hands, yields of **RV-29** were low (<40%) and contained impurities after column chromatography (data not shown). **RV-27** also appeared to be unstable (60-96%, n=6), with new impurities forming upon subsequent solvent removal *in vacuo* as determined by NMR. The cell viability of **RV-27** in U2OS SETD2 (+/+) and (-/-) cells was examined, but due to the perceived instability this data was not included in the analysis. In comparison to **RV-27** and **RV-28**, **RV-3** in comparison was obtained in relatively poor yield (14%) using the same method.

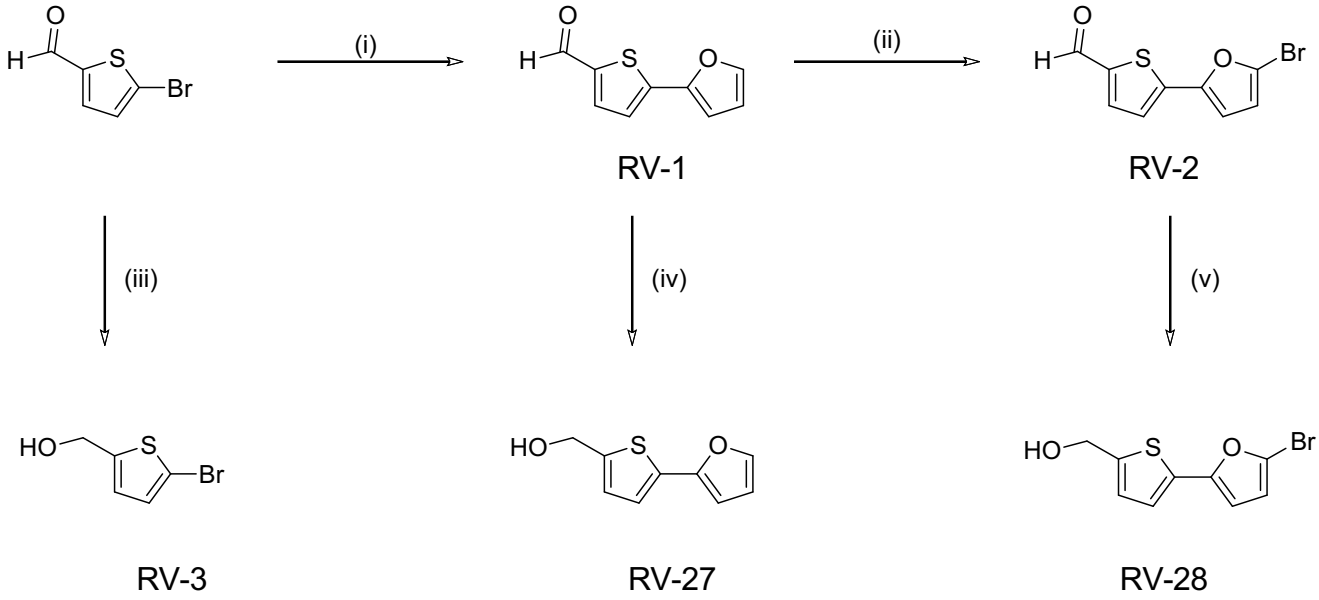

Scheme S2. Synthesis of aldehyde RITA starting materials. Reagents and conditions i) XPhos, $Pd(OAc)_2$, $MeCN/H_2O$ 3:2, 24 h, 24-70%, n=7; ii) NBS, BPO, Toluene, overnight, 49-70%, n=7; iii) $NaBH_4$ (0.5 eq.), $MeOH/CH_2Cl_2$ (1:1), 0 °C, 14% n=1; iv) $NaBH_4$ (0.5 eq.), $MeOH/CH_2Cl_2$ (1:1), 0 °C, 60-96%, n=6; v) $NaBH_4$ (0.5 eq.), MeOH/THF (1:1), 0 °C, yield generally assumed 100%

The dialdehyde compound **RV-6** was prepared from 5-(5-Bromofuran-2-yl)thiophene-2-carbaldehyde (**RV-2**) (Scheme S3). The equivalents of Xphos (0.04 eq.) and $Pd(OAc)_2$ (0.02 eq.) were increased compared to the initial conditions from Lin *et al.*[2] and the reaction carried out in degassed DMF, but similarly to Lin *et al.* this reaction resulted in low yields (13%). Lin *et al.*[2] identified that one of the major side products of this reaction is homocoupling of 5-formyl thiophene-2-boronic acid to give **RV-13**. We did not attempt to isolate **RV-13** in this reaction but it is likely that this is one of the major side products. In addition, it was noted that these type of compounds are generally poorly ionisable in ESI mass spectrometry, it is was only *via* HRMS that the product can be identified.

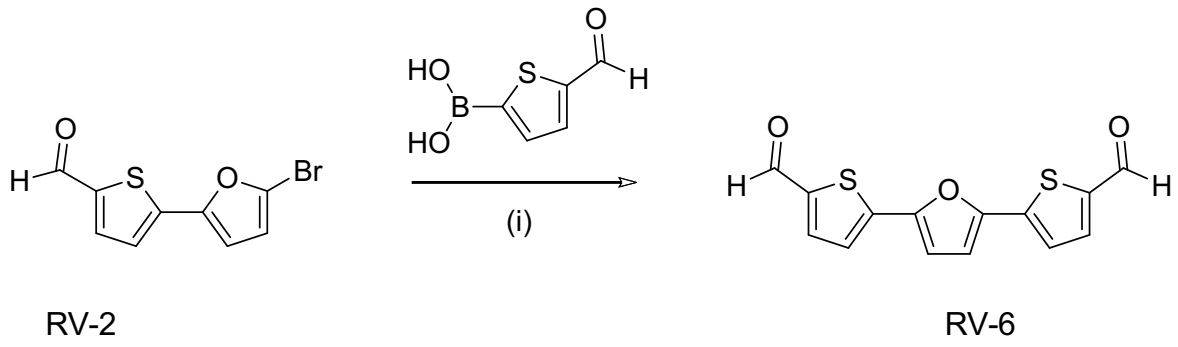

RV-2 RV-6

Scheme S3. Suzuki coupling of **RV-2** to give 2,5-bis(5-formylthiophen-2-yl)furan. **(RV-6)** (i) XPhos (0.04 eq.), $Pd(OAc)_2$ (0.02 eq.), DMF, 18 h, rt, 13%

Dialdehyde dyad **RV-13** was prepared from 5-bromo-thiophene-2-carbaldehyde and 5-formylthiophene-2-boronic acid (Scheme S4) using optimised XPhos (0.04 eq) and $Pd(OAc)_2$ (0.02 eq.) conditions in DMF with K_2CO_3 (3 eq.), resulting in a strong yellow solid, still in quite a low yield (28-50%, n=2). Dyad **RV-13** was reduced to dialcohol dyad **RV-14** using $NaBH_4$ in low yield (12%) (Scheme S4).

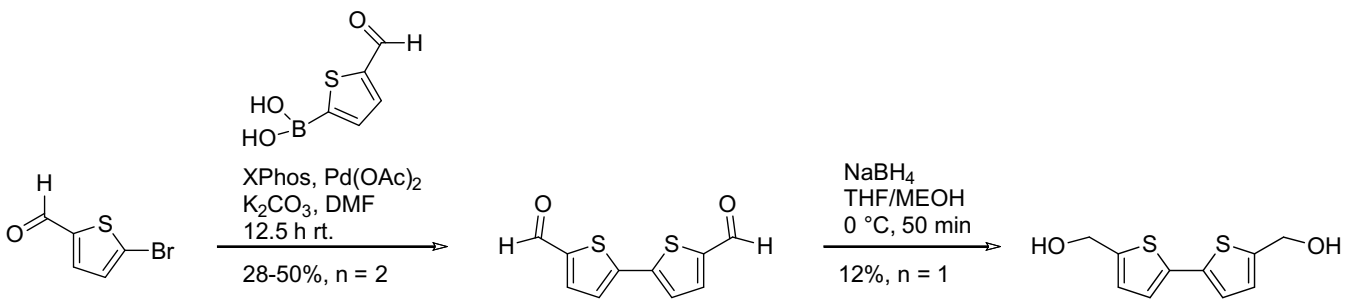

RV-13 RV-14

Scheme S4. Dyad **RV-13** and **RV-14** compound synthesis.

5-bromo-2-thiophene methyl ester **RV-7** was prepared by fisher esterification following a procedure by Kranich *et al.*[15] 5-Bromo-2-thiophenecarboxylic acid (1 eq.) was combined with H_2SO_4 (1 eq.) in methanol and the reaction stirred under reflux for 24 h (Scheme S5). **RV-7** was isolated *via* a basic work-up as a yellow oil that crystallised upon standing. No further purification was required (64-87%, n=4). These conditions were transferred to 5-di(hydroxybenzyl)-2-thiophenecarboxylic acid to give [5-(methyoxycarbonyl)thiophen-2-yl)boronic acid **RV-10** as a pale pink/orange solid (19-47%, n=2). A reduction in yield was expected for the boronic acid compared to the halogenated starting material as basic work-up would deprotonate the boronic acid, resulting in a majority of the product in the aqueous layer. Increasing the organic washing of the basic aqueous layer resulted in an increased yield (from 19% to 47%).

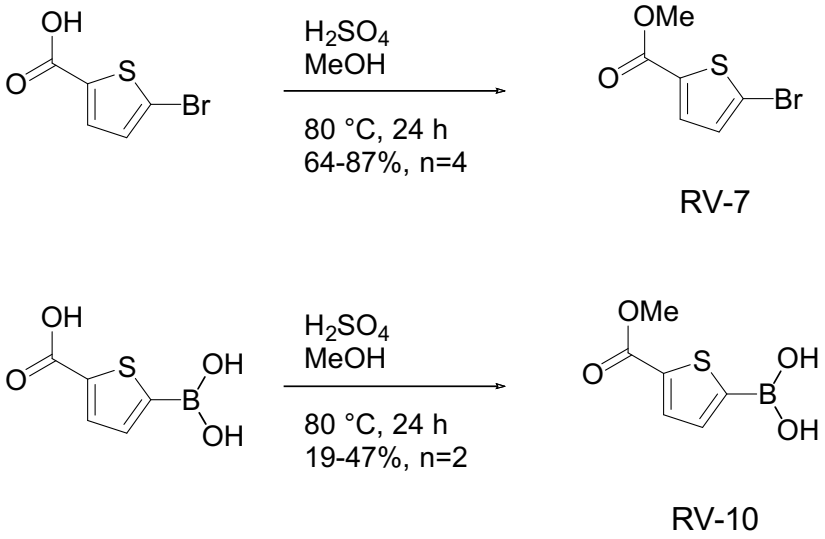

Scheme S5. Fisher esterification of thiophene carboxylic acids

It was proposed that the diester **RV-12** could be prepared *via* two methods (Scheme S6). Route A has the advantage that both the dual methyl ester **RV-12** and the mixed aldehyde/ester analogue **RV-11** are made from common intermediate methyl 5-(5-bromofuran-2-yl)thiophene-2-carboxylate (**RV-9**).

Initially following route A (Scheme S6), 5-bromo-2-thiophene methyl ester **RV-7** was combined in degassed MeCN/H_2O (1.5:1) with XPhos (0.04 equiv) and $Pd(OAc)_2$ (0.02 equiv) and K_2CO_3 (3 equiv) before 2-furanylboronic acid (1.3 equiv) was added and the reaction was allowed to stir at room temperature overnight to give methyl 5-(furan-2-yl)thiophene-2-carboxylate (**RV-8**) in poor to moderate yield (n=3, <10%-37%). It was considered that in a MeCN/H_2O solvent system, hydrolysis could occur on the methyl ester. The solvent was optimised on a 0.23 mmol scale, finding that the reaction proceeded poorly in toluene and isopropyl alcohol, but DMF resulted in improved yields of **RV-8** compared to MeCN/H_2O (48 and 28% respectively) (data not shown). When repeating this reaction on a larger scale in DMF (1 g, 4.5 mmol with 1.2 eq. of **RV-8**), the highest yield of 57% was obtained (data not shown).

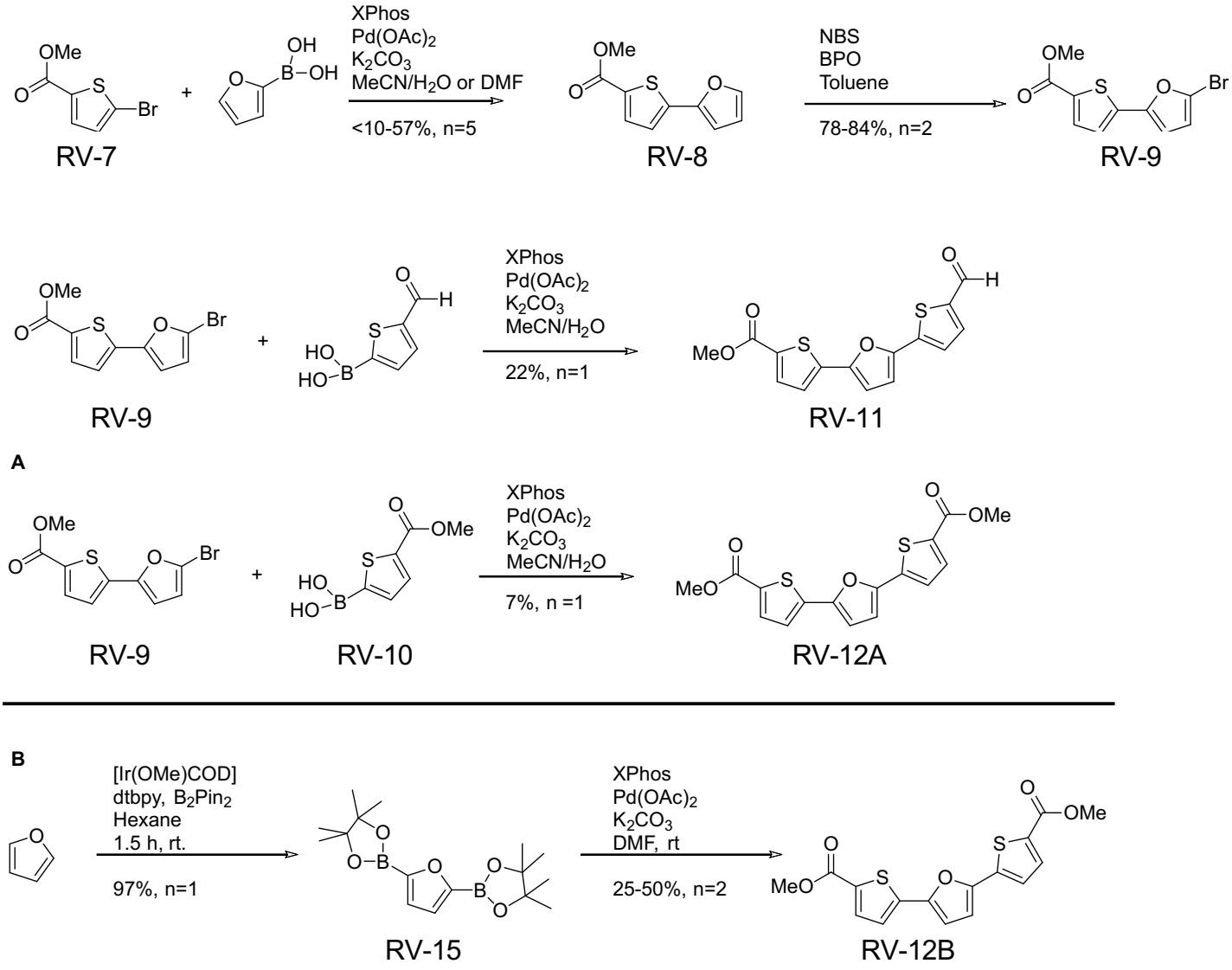

Scheme S6. Methods to create diester variant **RV-12** and mixed aldehyde/ester RV-11. RV-12 was prepared using two routes, route A and B.

Methyl 5-(5-bromofuran-2-yl)thiophene-2-carboxylate (**RV-9**) was prepared similarly to 5-(5-bromofuran-2-yl)thiophene-2-carbaldehyde (**RV-2**) described above. Methyl 5-(furan-2-yl)thiophene-2-carboxylate (**RV-8**) (1 eq.) was combined with benzoyl peroxide (0.015 eq.) in toluene in the dark and the reaction was cooled to – 23 °C before n-bromosuccinimide (1 eq.) was added portionwise over 30 minutes. This reaction proceeded smoothly giving methyl 5-(5-bromofuran-2-yl)thiophene-2-carboxylate (**RV-9**) in high yield (78-84%, n=2).

For the mixed diester/dialdehyde analogue **RV-11**, methyl 5-(5-bromofuran-2-yl)thiophene-2-carboxylate (**RV-9**) (1 eq.) was combined in degassed $MeCN/H_2O$ (1.5:1) with XPhos (0.04 eq.), $Pd(OAc)_2$ (0.02 eq.) and K_2CO_3 (3 eq.) before 5-formyl-2-thienylboronic acid (1.5 eq.) was added and the reaction was allowed to stir at room temperature overnight under argon.

To remove ^{1}H grease (Fulmer *et al.*[16]), the product was dissolved in CH_2Cl_2 (20 mL) and washed several times with hexane and the product reisolated as a yellow powder (22%). Dimethyl 5,5'-(furan-2,5-diyl)bis(thiophene-2-carboxylate) (**RV-12**) was prepared similarly from **RV-9** which was combined with XPhos (0.04 eq.), $Pd(OAc)_2$ (0.02 eq.) and K_2CO_3 (3 eq.) before 5-formyl-2-thienylboronic acid (1.5 eq.) **RV-10** was added (1.5 eq.). This compound required two column purifications and resulted in a very low yield (7%).

Due the poor yield obtained, we next attempted to synthesize **RV-12** via route B (Scheme S6). 2,5-bis(4,4,5,5-tetramethyl-1,3,2-dioxaborolan-2-yl)furan (**RV-15**) was prepared from furan as per Ishiyama *et al.* with minor modifications to the work-up procedure and was used without further purification (97%).[17] Using the optimised Suzuki coupling conditions in degassed DMF, the amount of K_2CO_3 (6 eq.), XPhos (0.08 eq.) and $Pd(OAc)_2$ (0.04 eq.) was doubled. Compound **RV-15** was combined with **RV-7** and the reaction left to stir at room temperature overnight. Although this procedure could require two column purifications also, the yield was much higher between 25-50% (n=2).